

$^2\text{H}(e, e'p)n$ Reaction at High Recoil Momenta

P. E. Ulmer,¹ K. A. Aniol,² H. Arenhövel,³ J.-P. Chen,⁴ E. Chudakov,⁴ D. Crovelli,⁵ J. M. Finn,⁶ K. G. Fissum,⁷ O. Gayou,^{6,8} J. Gomez,⁴ J.-O. Hansen,⁴ C. W. de Jager,⁴ S. Jeschonnek,^{4,9} M. K. Jones,¹ M. Kuss,⁴ J. J. LeRose,⁴ M. Liang,⁴ R. A. Lindgren,¹⁰ S. Malov,⁵ D. Meekins,¹¹ R. Michaels,⁴ J. Mitchell,⁴ C. F. Perdrisat,⁶ V. Punjabi,¹² R. Roché,¹¹ F. Sabatie,¹ A. Saha,⁴ R. Suleiman,¹³ L. Todor,¹ and B. B. Wojtsekhowski⁴

¹Old Dominion University, Norfolk, Virginia 23529

²California State University at Los Angeles, Los Angeles, California 90032

³Johannes Gutenberg-Universität, D-55099 Mainz, Germany

⁴Thomas Jefferson National Accelerator Facility, Newport News, Virginia 23606

⁵Rutgers, The State University of New Jersey, Piscataway, New Jersey 08855

⁶College of William and Mary, Williamsburg, Virginia 23187

⁷University of Lund, P.O. Box 118, SE-221 00 Lund, Sweden

⁸Université Blaise Pascal/CNRS-IN2P3, F-63177 Aubière, France

⁹The Ohio State University, Lima, Ohio 45804

¹⁰University of Virginia, Charlottesville, Virginia 22901

¹¹Florida State University, Tallahassee, Florida 32306

¹²Norfolk State University, Norfolk, Virginia 23504

¹³Kent State University, Kent, Ohio 44242

(Received 20 November 2001; published 19 July 2002)

The $^2\text{H}(e, e'p)n$ cross section was measured in Hall A of the Thomas Jefferson National Accelerator Facility near the top of the quasielastic peak ($x_{Bj} = 0.964$) at a four-momentum transfer squared, $Q^2 = 0.665 \text{ (GeV}/c)^2$ ($\omega = 0.368 \text{ GeV}$, $W = 2.057 \text{ GeV}$), and for recoil momenta up to $550 \text{ MeV}/c$. The measured cross section deviates by $1\text{--}2\sigma$ from a state-of-the-art calculation at low recoil momenta. At high recoil momenta the cross section is well described by the same calculation; however, in this region, final-state interactions and interaction currents are predicted to be large, and alternative choices of nucleon-nucleon potential and nucleon current operator may result in significant spread in the calculations.

DOI: 10.1103/PhysRevLett.89.062301

PACS numbers: 25.30.Fj, 21.30.-x, 21.45.+v

There exists a wealth of precision data on nucleon-nucleon (NN) scattering below the π -production threshold [1], which is well described by modern potential models for the NN interaction [2–5]. These models differ in their short-range structure predicting different high-momentum components of the deuteron wave function. It is therefore highly desirable to perform measurements on the deuteron in kinematics where its short-distance structure is emphasized. The $^2\text{H}(e, e'p)n$ reaction is an ideal candidate for such studies since the final state is completely specified kinematically and one can tune the kinematics to emphasize high-momentum components in the deuteron wave function. However, extracting information on the deuteron's structure requires a quantitative understanding of the reaction dynamics. In this Letter, we report a measurement of the $^2\text{H}(e, e'p)n$ cross section at Jefferson Lab (JLab) which serves as a test of reaction models in a hitherto inaccessible kinematic regime.

In the simplest picture of the $^2\text{H}(e, e'p)n$ reaction, the plane wave impulse approximation (PWIA), a proton is knocked out by the virtual photon and is detected without any further interaction with the unobserved neutron. In this picture, the cross section is related to the nucleon momentum distribution, and the kinematically determined final-state neutron momentum, referred to here as the “recoil”

momentum (p_r), is simply the negative of the initial proton momentum. The actual reaction mechanism is much more complicated, and includes hadronic rescattering in the final state [final state interactions (FSI)] and two-body currents [meson exchange currents (MEC), and isobar configurations (IC)]. Information on the deuteron's short-distance structure can be gained only in the context of reaction models which include a quantitative description of such complications.

Accessing the deuteron's short-range structure implies measurements at large values of p_r . Our experiment was performed in the “perpendicular kinematics” configuration. Here, the electron kinematics are fixed at the quasielastic peak ($x_{Bj} \equiv Q^2/2m\omega \approx 1$ where $Q^2 = |\vec{q}|^2 - \omega^2$, \vec{q} , and ω are the momentum and energy of the virtual photon and m is the proton mass) and a range of p_r is obtained by measuring the angular distribution of protons about \vec{q} . In this kinematic configuration, FSI can change the cross section at high p_r by a sizable amount (see Ref. [6] and also Fig. 1 below). These large effects result from the rapid falloff of the wave function coupled with the feeding of strength from low initial momentum to high p_r due to np rescattering. The effects of two-body currents are also expected to be significant at high p_r . Thus, this experiment will help constrain these model dependencies

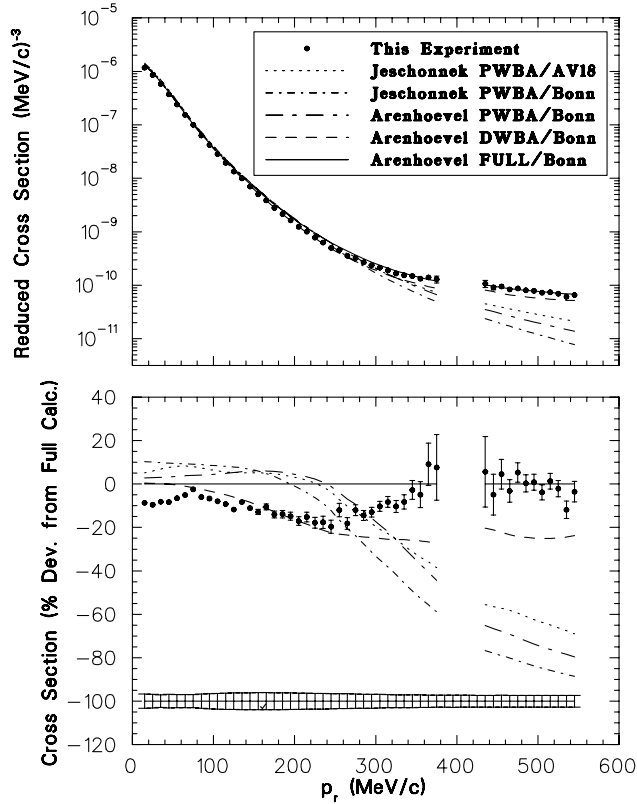


FIG. 1. Top panel: The reduced ${}^2\text{H}(e, e'p)n$ cross section for this experiment, along with various model calculations. The calculations of Jeschonnek were performed with both the Argonne V18 (AV18) and Bonn NN potentials, whereas the calculations of Arenhoevel used only the Bonn potential (see the text for more details). Bottom panel: Cross sections for data and calculations shown as percentage deviations from the full calculation of Arenhoevel. Also shown is the systematic error band ($\pm 1\sigma$), arbitrarily placed on the vertical axis. This error band contains only point-to-point sources; the overall scale uncertainty of 6.8% is not included.

in a kinematic region where they have large effects. Models which succeed under such stringent tests may then be applied with some confidence to infer aspects of the deuteron short-distance structure in the “parallel kinematics” configuration (i.e., protons detected along \vec{q}) where p_r can be large while influences from FSI and two-body currents are expected to be minimized [7].

There is a substantial body of data for the ${}^2\text{H}(e, e'p)n$ reaction, including cross-section measurements [8–11] as well as separations of various response functions [12–21] which differentiate between absorption of longitudinal and transverse photons. However, truly systematic studies of this reaction have been hindered by limitations of the various accelerators. For example, accelerator energy limitations forced the Turck-Chieze [9] and high p_r Mainz [11] data to be taken in the Δ region of the inclusive (e, e') spectrum where lack of knowledge of the reaction mechanism made it difficult to deduce aspects of the deuteron

structure. Further, although the Mainz measurement sampled p_r up to 928 MeV/c, the kinematics actually imply that the bulk of the cross section arises from interaction with the neutron, leaving the detected proton as a spectator. Although the energy limitation is not shared by SLAC, the maximum current and duty factor restricted the range of recoil momenta there as well. In contrast, JLab finally allows a thorough examination of the reaction over a broad kinematic range. Our data represent the first component of such a study wherein JLab’s unique combination of high energy, duty factor, and beam current allowed the measurement to be carried out at both high p_r and high Q^2 , while fixing x_{Bj} on the quasielastic peak. While Q^2 is relatively high compared to previous measurements, its value was chosen to lie within the range where relativistic effects can be treated via an approximate scheme and where, therefore, current theories are within their expected range of validity.

Our experiment consisted of measuring the ${}^2\text{H}(e, e'p)n$ cross section out to high p_r . It was performed in Hall A of JLab using the high resolution spectrometer pair. A detailed description of the Hall A instrumentation is currently being prepared [22]. Electrons from the accelerator were incident on a 15 cm long liquid deuterium target. Scattered electrons and knockout protons were detected in the high resolution spectrometers, each with a nominally 6.0 msr collimator at its front end. The spectrometers were equipped with their standard detector packages consisting of a pair of vertical drift chambers (VDC’s) for track reconstruction and a scintillator array for trigger definition. In addition, the electron spectrometer included an atmospheric pressure CO_2 threshold Čerenkov detector for π^-/e discrimination.

Kinematics were centered roughly on the quasielastic peak with $x_{Bj} = 0.964$ and $Q^2 = 0.665$ (GeV/c) 2 . The beam energy as well as the angle and central momentum of the electron spectrometer were kept fixed throughout the experiment at values of 3.110 GeV, 16.06° and 2.742 GeV/c, respectively, giving $\omega = 0.368$ GeV and a final-state, center-of-mass hadronic energy of $W = 2.057$ GeV. The recoil momentum was varied by changing the proton spectrometer angle starting from the \vec{q} direction where $p_r = 0$ to more backward angles resulting in a maximum central value of $p_r = 500$ MeV/c. The proton angle (momentum) relative to the incident electron direction varied from 58.76° (0.885 GeV/c) to 92.78° (0.689 GeV/c), with all quantities expressed in the laboratory system. Obstruction from one of the scattering chamber support posts resulted in a fairly wide spacing between two of the settings and a gap in the measured spectrum vs p_r .

Measurement of the elastic ${}^1\text{H}(e, e'p)$ reaction, taken with the spectrometers at the ${}^2\text{H}(e, e'p)n$ $p_r = 0$ setting, served as a normalization check. The measured yield was compared to a simulation [23] using the Simon *et al.* [24] parametrization for G_{M_p} and the G_{E_p}/G_{M_p} ratio measured

by Jones *et al.* [25], where G_{M_p} and G_{E_p} are the Sachs magnetic and electric form factors of the proton, respectively. The simulation included acceptance averaging as well as radiative folding [26]. In order to remove the ill-defined acceptance edges a technique involving “ R functions” [27] was used. Through the R functions, a multi-dimensional contour in the space of the target variables and equidistant from a predefined boundary was defined and all events outside the contour were rejected. The same contour was used in the simulations and for the $^1\text{H}(e, e'p)$ and $^2\text{H}(e, e'p)n$ data. The ratio of integrated yield for the simulation to that for the $^1\text{H}(e, e'p)$ data was 1.054, amounting to a 5.4% correction for the $^2\text{H}(e, e'p)n$ data.

For the $^2\text{H}(e, e'p)n$ data, beam currents ranged from 10 to 100 μA . Since the electron kinematics were fixed, the electron arm served as a measure of the product of electronic deadtime and target density; the electronic deadtime for the hadron arm was assumed to be negligible, since its trigger rate never exceeded 10 kHz. Computer deadtime was determined from the ratio of coincidence raw triggers to recorded events. In order to improve the “reals-to-accidentals” ratio, especially important at high p_r , a consistent vertex from both spectrometers was required and a cut on the missing mass was imposed. Finally, a cut on the summed analog signal from the Čerenkov detector was used to reduce the already small contamination from π^- events in the electron arm. The aperture/magnetic model of each spectrometer was tested by measuring a series of “white” spectra, scanned in overlapping momentum steps. The relative spectrometer acceptance was then extracted by an iterative procedure. For the R -function cuts described above, the results were in excellent agreement with the simulated phase space.

The systematic uncertainties in the cross sections can be divided into three classes. The first class consists of overall scale uncertainties which total 6.8% in quadrature: electron arm solid angle (2.0%), radiative correction (3.0%), and $^1\text{H}(e, e'p)$ normalization (5.8%). Note that the electron solid angle uncertainty is not removed by scaling to the normalization measurement since the hadron arm limited the acceptance in that case. The second class consists of point-to-point uncertainties which total 2.4%: electronic deadtime \times target density (2.0%), beam charge (1%), and proton arm solid angle (1%). Note that the beam charge and proton arm solid angle uncertainties are relative only as the absolute errors have already been accounted for via the $^1\text{H}(e, e'p)$ normalization. The third class consists of p_r dependent kinematic uncertainties. They were estimated by simulating the yields in each bin in p_r for the nominal kinematics and for variations of each of the kinematic quantities. The quantities were varied in a correlated fashion, constrained by the elastic $^1\text{H}(e, e'p)$ kinematics and by independent measurement of the beam energy, obtained by measuring the position of the beam at a point of high dispersion in an eight dipole arc section. The quadrature sum for the kinematics uncertainties was less

than 3.1% for all recoil momenta. As these uncertainties depend on p_r , we treat them as point to point and thus take the total point-to-point uncertainty to be the quadrature sum of uncertainties from the second and third classes.

The results for data along with various calculations are shown in Fig. 1. The top panel shows the radiatively corrected “reduced” cross section:

$$\sigma_{\text{red}} \equiv \frac{d^5\sigma}{d\Omega_e d\omega d\Omega_p} \times \frac{1}{f_{\text{rec}} K \sigma_{\text{CC1}}},$$

where K is a kinematic factor, σ_{CC1} is the half-off-shell electron-proton cross section of de Forest [28], and f_{rec} is a recoil factor which arises from the integration over missing mass. This division removes most of the kinematic dependence, except for the p_r dependence, and results in a relatively smooth spectrum vs p_r . The bottom panel shows the deviation of data and the various theoretical predictions from the full calculation of Arenhövel [29] (described below). Also shown in the bottom panel is the systematic error band (point-to-point sources only), arbitrarily placed vertically. The data were radiatively corrected by multiplying the measured cross section in each p_r bin by the ratio of yield without and with radiative effects (internal and external), estimated using Arenhövel’s full calculation and folded using the model of Borie and Drechsel [30].

All of the models were acceptance averaged using MCEEP [23]; the calculations of Jeschonnek [31] were incorporated directly into the Monte Carlo simulation program as a subroutine package, whereas those of Arenhövel were performed on a grid over the experimental acceptance and interpolated for each event. The calculations as reported in [6] employ Glauber theory to describe the FSI, which is strictly valid only for energy transfers above 1 GeV. As our data are not in this regime, the Jeschonnek calculations presented in this paper are strictly within the framework of the relativistic plane wave Born approximation [(PWBA), which includes scattering from the neutron as well as the proton]. A fully relativistic single-nucleon current operator with an alternate three-pole parameterization of the Mergell-Meissner-Drechsel nucleon form factors [32] and the Argonne V18 [4] as well as the Bonn [2] two-body interaction were used. The calculations of Arenhövel included relativistic contributions of leading order in p/m to the kinematic wave function boost and to the nucleon current. The Bonn potential and dipole nucleon form factors were used. The various curves are for PWBA, distorted wave Born approximation (which includes FSI), and the full calculation which also includes non-nucleonic currents: MEC and IC.

For $p_r < 300$ MeV/ c the full theory deviates from the data by roughly 1–2 σ , adding statistical and all systematic errors quadratically. The oscillation of the data relative to Arenhövel’s full calculation in this region of p_r cannot be accommodated by the level of point-to-point uncertainties. It is important to resolve such discrepancies, especially in

light of some of the neutron form factor measurements which exploit the deuteron in this kinematic region. Discrepancies at low p_r have also been observed in other $^2\text{H}(e, e'p)n$ experiments [8,14]. For $p_r > 300 \text{ MeV}/c$ the PWBA fails completely, whereas the full calculation including FSI and significant contributions from non-nucleonic degrees of freedom results in satisfactory agreement with the data. The difference between the two relativistic PWBA/Bonn calculations grows with p_r , indicating sensitivity to the treatment of relativity and/or the choice of nucleon current operator. The difference between the Jeschonnek PWBA curves for the Argonne V18 and the Bonn potentials also grows with p_r , indicating sensitivity to the choice of NN potential as well. It remains to be seen whether these model dependences persist when interaction currents are included in the other approaches. In other words, it is at present an open question whether the agreement seen at high p_r is fortuitous or not.

In summary, we have measured the $^2\text{H}(e, e'p)n$ cross section at $Q^2 = 0.665 (\text{GeV}/c)^2$ and $x_{Bj} = 0.964$ for recoil momenta up to $550 \text{ MeV}/c$. At high p_r , theoretical results in PWBA fail to describe the data whereas the full calculation with inclusion of FSI and subnucleonic effects leads to considerable improvement though not perfect agreement. However, the full calculation overestimates the cross section by $1\text{--}2\sigma$ at small recoil momenta. Given the level of model dependences demonstrated here, it would be highly desirable to carry out additional measurements [33] where various model sensitivities are separately emphasized.

We acknowledge the outstanding support of the staff of the Accelerator and Physics Divisions at Jefferson Laboratory that made this experiment successful. We also thank Robert Lourie for useful discussions. This work was supported in part by the U.S. Department of Energy Contract No. DE-AC05-84ER40150 under which the Southeastern Universities Research Association (SURA) operates the Thomas Jefferson National Accelerator Facility, other Department of Energy contracts, the U.S. National Science Foundation, the French Commissariat à l'Energie Atomique and Centre National de la Recherche Scientifique (CNRS), the Deutsche Forschungsgemeinschaft (SFB 443) and the Swedish Natural Science Research Council.

-
- [1] R. Machleidt and I. Slaus, *J. Phys. G* **27**, R69 (2001); nucl-th/0101056.
 - [2] R. Machleidt, K. Holinde, and Ch. Elster, *Phys. Rep.* **149**, 1 (1987).

- [3] M. Lacombe *et al.*, *Phys. Lett.* **101B**, 139 (1981).
- [4] R. B. Wiringa, V. G. J. Stoks, and R. Schiavilla, *Phys. Rev. C* **51**, 38 (1995).
- [5] V. G. J. Stoks, R. A. M. Klomp, M. C. M. Rentmeester, and J. J. de Swart, *Phys. Rev. C* **48**, 792 (1993).
- [6] S. Jeschonnek and T. W. Donnelly, *Phys. Rev. C* **59**, 2676 (1999).
- [7] W. Fabian and H. Arenhövel, *Nucl. Phys.* **A314**, 253 (1979).
- [8] M. Bernheim *et al.*, *Nucl. Phys.* **A365**, 349 (1981).
- [9] S. Turck-Chieze *et al.*, *Phys. Lett.* **142B**, 145 (1984).
- [10] H. Breuker *et al.*, *Nucl. Phys.* **A455**, 641 (1986).
- [11] K. I. Blomqvist *et al.*, *Phys. Lett. B* **424**, 33 (1998).
- [12] M. van der Schaar *et al.*, *Phys. Rev. Lett.* **68**, 776 (1992).
- [13] T. Tamae *et al.*, *Phys. Rev. Lett.* **59**, 2919 (1987).
- [14] M. van der Schaar *et al.*, *Phys. Rev. Lett.* **66**, 2855 (1991).
- [15] F. Frommberger *et al.*, *Phys. Lett. B* **339**, 17 (1994).
- [16] J. E. Ducret *et al.*, *Phys. Rev. C* **49**, 1783 (1994).
- [17] H. J. Bulten *et al.*, *Phys. Rev. Lett.* **74**, 4775 (1995).
- [18] D. Jordan *et al.*, *Phys. Rev. Lett.* **76**, 1579 (1996).
- [19] A. Pellegrino *et al.*, *Phys. Rev. Lett.* **78**, 4011 (1997).
- [20] W.-J. Kasdorp *et al.*, *Phys. Lett. B* **393**, 42 (1997).
- [21] Z.-L. Zhou *et al.*, *Phys. Rev. Lett.* **87**, 172301 (2001).
- [22] B. D. Anderson *et al.*, "Basic Instrumentation for Hall A at Jefferson Lab," *Nucl. Instrum. Methods* (to be published).
- [23] P. E. Ulmer, computer program MCEEP, "Monte Carlo for $(e, e'p)$ Experiments," JLAB Technical Note No. 91-101 (1991).
- [24] G. G. Simon *et al.*, *Nucl. Phys.* **A333**, 381 (1980).
- [25] M. K. Jones *et al.*, *Phys. Rev. Lett.* **84**, 1398 (2000).
- [26] L. W. Mo and Y. S. Tsai, *Rev. Mod. Phys.* **41**, 205 (1969).
- [27] V. L. Rvachev, T. I. Sheiko, V. Shapiro, and I. Tsukanov, *Comp. Mech.* **25**, 305 (2000).
- [28] T. de Forest, Jr., *Nucl. Phys.* **A392**, 232 (1983).
- [29] H. Arenhövel (private communication); W. Leidemann, E. L. Tomusiak, and H. Arenhövel, *Phys. Rev. C* **43**, 1022 (1991); H. Arenhövel, W. Leidemann, and E. L. Tomusiak, *Phys. Rev. C* **46**, 455 (1992); *Phys. Rev. C* **52**, 1232 (1995); F. Ritz, H. Göller, Th. Wilbois, and H. Arenhövel, *Phys. Rev. C* **55**, 2214 (1997).
- [30] E. Borie and D. Drechsel, *Nucl. Phys.* **A167**, 369 (1971).
- [31] S. Jeschonnek (private communication); S. Jeschonnek and T. W. Donnelly, *Phys. Rev. C* **57**, 2438 (1998); S. Jeschonnek and J. W. Van Orden, *Phys. Rev. C* **62**, 044613 (2000).
- [32] J. W. Van Orden (private communication); P. Mergell, Ulf-G. Meissner, and D. Drechsel, *Nucl. Phys.* **A596**, 367 (1996).
- [33] W. Boeglin, M. Jones, A. Klein, P. E. Ulmer, and E. Voutier, cospokespersons, " $(e, e'p)$ Studies of the Deuteron at High Q^2 ," JLAB proposal No. E01-020.